

RETROGRADE SOLUBILITIES OF SOURCE TERM PHASES

WILLIAM M. MURPHY

Center for Nuclear Waste Regulatory Analyses, Southwest Research Institute,
6220 Culebra Road, San Antonio, TX 78228-0510 USA

ABSTRACT

Natural analog, experimental, and thermodynamic studies indicate that the properties of secondary uranyl minerals are likely to control the source term for U and other radioelements incorporated in these phases in the proposed Yucca Mountain repository. Thermodynamic calculations using data from the 1992 NEA data base indicate an increase in the equilibrium constant for schoepite dissolution from $10^{3.1}$ to $10^{4.8}$ with decreasing temperature from 100° to 25°C, i.e., retrograde solubility. Enthalpies for mineral transformation reactions that consume protons and release cations are typically negative, suggesting that solubilities of other uranyl phases such as uranophane increase more than that of schoepite with decreasing temperature. Solubilities of mineral phases associated with spent nuclear fuel will be initially relatively low under the elevated repository temperature regime. As the temperature of the repository decreases due to radioactive decay and heat dissipation, source term mineral solubilities increase. The rate of release of U and other species is controlled by a series of processes: transport of oxidants and flux of water; oxidative dissolution of spent fuel; uranyl mineral precipitation; uranyl mineral dissolution or transformation; and radionuclide transport. Decreasing diffusion and reaction rates and increasing uranyl mineral solubilities with decreasing temperature may lead to a change with time from solubility to transport or reaction rate as a source term controlling mechanism. Preservation of large quantities of uranyl minerals formed by oxidation of uraninite and radiometric ages of secondary uranophane at the natural analog site at Peña Blanca indicate that oxidative alteration of uraninite was fast relative to transport of U away from the deposit. The successive formation of schoepite and uranophane in natural settings where uraninite has been oxidized may represent a paragenesis reflecting increasing temperature or increasing incorporation of environmental components. In contrast, diminishing temperature conditions in a repository source area could lead to the reverse sequence of mineral formation.

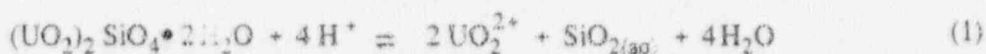
INTRODUCTION

It is widely recognized from theoretical, experimental, and natural analog studies related to the oxidizing environment at Yucca Mountain that secondary minerals, particularly those containing uranyl, are likely to play an important role in controlling the source term for U and much of the inventory of nuclear waste, e.g., [1], [2]. Furthermore, after a few tens of years following emplacement, the continuously decreasing temperature of the source area at the proposed repository will affect differentially the properties of secondary phases and the processes that lead to radionuclide release. Nevertheless, little recognition of the role of secondary uranyl minerals or the relative temperature dependence of solubilities and reaction rates is acknowledged in source term analyses for performance assessments. This article examines thermodynamic data for likely secondary uranyl phases to support realistic predictions of their role in the evolution of the source term and ultimately the performance of the proposed repository. In particular, the temperature dependence of uranyl mineral solubilities is examined and implications are developed for their role as source term phases and for the application of natural analog data to predictions of repository performance.

SOLUBILITY DATA

Limited empirical thermodynamic data exist for uranyl minerals particularly above 25°C. Properties for the uranyl hydrate, with the nominal composition of schoepite¹ ($\text{UO}_3 \cdot 2\text{H}_2\text{O}$), are recommended in the recently published, comprehensive review of chemical thermodynamics of U by Grenthe et al. [3]. These data are derived from calorimetric studies, primarily by Tasker et al. [4]. Attempts have been made to determine equilibrium solubilities of uranyl minerals using synthetic and natural samples [5], [6], [7], [8]. However, principal problems in these solubility experiments and data interpretations are: reaction stoichiometries were not firmly ascertained; chemical formulas used in thermodynamic interpretations were inconsistent with analytical data; phases other than those of primary interest were present as contaminants or precipitates and demonstrably affected some results; and solubility reversals were not attempted. Reversed solubility measurements of schoepite of unknown hydration at 90°C have been determined [8], but complete solution compositions were unspecified and no thermodynamic interpretation was reported.

Dissolution studies for soddyite [5], [7] provide the most likely basis for retrieval of reliable thermodynamic data for a uranyl silicate mineral. However, it was assumed in these studies that the soddyite conformed to its nominal ideal stoichiometry. In one study [5] excess Si detected in the reactant material and deficit silica in solution were assumed to be a consequence of the initial presence and experimental precipitation of amorphous silica, respectively. For the soddyite dissolution reaction



the corresponding equilibrium constant is defined by

$$K_{\text{sod}} = \frac{[\text{UO}_2^{2+}]^2 [\text{SiO}_{2(\text{aq})}] [\text{H}_2\text{O}]^4}{[(\text{UO}_2)_2\text{SiO}_4 \cdot 2\text{H}_2\text{O}] [\text{H}^+]^4} \quad (2)$$

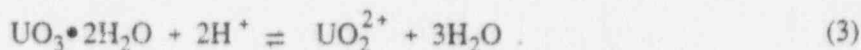
where square brackets represent thermodynamic activities corresponding to standard state of a one molal solution referenced to infinite dilution for aqueous species and pure minerals and H_2O . Thermodynamic data reported for reaction (1) are $\log K_{\text{sod}} = 5.74 \pm 0.21$ at 30°C, and the corresponding standard free energy of formation of soddyite from the elements, $\Delta G_f^\circ_{\text{sod}} = -3.658 \pm 4.8 \text{ kJ} \cdot \text{mole}^{-1}$ [5]. (Reported uncertainties are based on uncertainties in standard state properties for the aqueous species and H_2O and propagated standard deviations of analytical results.) However, equilibrium was approached only from undersaturation (i.e., the reaction was not reversed), so the solubility must be regarded as a lower limit. These results for soddyite solubility are supported by a dissolution solubility study of synthetic $(\text{UO}_2)_2\text{SiO}_4 \cdot 2\text{H}_2\text{O}$ at 25°C [7]. At pH 3, releases of UO_2^{2+} and $\text{SiO}_{2(\text{aq})}$ were generally in proportions corresponding to soddyite stoichiometry. However, mass balance relations indicate that silica (probably amorphous) began to precipitate prior to reaching soddyite solubility. The equilibrium constant deduced from the "steady state" solution compositions

¹Structural and compositional relations between schoepite, metaschoepite, and dehydrated schoepite have been detailed recently [9]. The phase corresponding to $\text{UO}_3 \cdot 2\text{H}_2\text{O}$ was classified as metaschoepite, and schoepite was characterized as having a higher degree of hydration. Reported calorimetric data [3] are for the crystalline uranyl hydrate, $\text{UO}_3 \cdot 2\text{H}_2\text{O}$, which is called schoepite in this article.

in the study is $\log K_{\text{sod}} = 6.03 \pm 0.45$, where the reported uncertainty is based on analytical uncertainties in pH and dissolved species concentrations. Although uncertainties are too large to confirm a trend in solubility with temperature between 25° and 30°C, the data from these two dissolution studies suggest retrograde solubility of soddyite (i.e., decreasing solubility with increasing temperature).

TEMPERATURE DEPENDENCE OF URANYL MINERAL SOLUBILITY

Reported thermodynamic data [3] permit evaluation of the solubility of schoepite as a function of temperature. Dissolution of schoepite is expressed as



The equilibrium solubility of schoepite is expressed by the mass action relation for reaction (3) as

$$K = \frac{[\text{UO}_2^{2+}][\text{H}_2\text{O}]^3}{[\text{UO}_3 \cdot 2\text{H}_2\text{O}][\text{H}^+]^2} \quad (4)$$

where K stands for the equilibrium constant for reaction (3). The temperature dependence of K is given by the van't Hoff relation

$$\frac{d \ln K}{dT} = \frac{\Delta H^\circ}{RT^2} \quad (5)$$

where T denotes temperature in kelvins, ΔH° stands for the standard state molar enthalpy of reaction, and R represents the ideal gas constant. The standard enthalpy of reaction as a function of temperature is given as the integral of the standard heat capacity of reaction (ΔC_p°)

$$\Delta H^\circ(T) - \Delta H^\circ(T^*) = \int_{T^*}^T \Delta C_p^\circ dT \quad (6)$$

where $\Delta H^\circ(T^*)$ stands for the standard enthalpy of reaction at the reference temperature (T^*).

$\Delta H_{298.15\text{K}}^\circ = -50.39 \pm 2.27 \text{ kJ} \cdot \text{mole}^{-1}$ for reaction (3) [3]. The heat capacity of reaction (3) is given by

$$\Delta C_p^\circ = 3C_{p,\text{H}_2\text{O}}^\circ + C_{p,\text{UO}_2^{2+}}^\circ - C_{p,\text{schoepite}}^\circ - 2C_{p,\text{H}^+}^\circ \quad (7)$$

where $C_{p,i}^\circ$ represents the standard molar heat capacity of species i . Using heat capacity functions and values from [3] for UO_2^{2+} (extrapolated above 328 K) and schoepite, and a constant heat capacity for H_2O of $75.48 \text{ J} \cdot \text{K}^{-1} \cdot \text{mole}^{-1}$, which is accurate within 1 percent between 25° and 100°C [10], the heat capacity of reaction (3) calculated using Eq. (7) is given by

$$\Delta C_p^\circ = 492.71 (\text{J} \cdot \text{K}^{-1} \cdot \text{mole}^{-1}) - 1.1668 (\text{J} \cdot \text{K}^{-2} \cdot \text{mole}^{-1}) T - \frac{5308 (\text{J} \cdot \text{mole}^{-1})}{T - 190 (\text{K})} \quad (8)$$

$$= A - B T - \frac{C}{T - D}$$

Using Eqs. (6) and (8), the integral of Eq. (5) yields the equilibrium solubility constant of schoepite as a function of temperature, which can be expressed as

$$\ln K - \ln K^\circ = \int_{T^\circ}^T \frac{\Delta H^\circ(T)}{RT^2} dT$$

$$= \int_{T^\circ}^T \left\{ \frac{A(T - T^\circ)}{RT^2} - \frac{B[T^2 - (T^\circ)^2]}{2RT^2} - \frac{C}{RT^2} \ln \left[\frac{T - D}{T^\circ - D} \right] + \frac{\Delta H^\circ(T^\circ)}{RT^2} \right\} dT \quad (9)$$

where K° denotes the equilibrium constant at T° . Using standard state free energies of formation of reactants and products in reaction (3) taken from [3] gives

$$K_{298.15} = \exp \left[\frac{-\Delta G_{(T^\circ)}}{RT} \right] = 6.50 \times 10^4 \quad (10)$$

where $\Delta G_{(T^\circ)}$ stands for the standard state Gibbs free energy of reaction (3) at 298.15 K. Solving the definite integral in Eq. (9) yields

$$\ln K - \ln K^\circ = \frac{A}{R} \ln \frac{T}{T^\circ} + \left[\frac{\Delta H^\circ(T^\circ) - A T^\circ}{R} + \frac{B(T^\circ)^2}{2R} \right] \left[\frac{1}{T^\circ} - \frac{1}{T} \right]$$

$$- \frac{B(T - T^\circ)}{2R} - \frac{C}{DR} \left[\frac{T - D}{T} \ln \left[\frac{T - D}{T^\circ - D} \right] + \ln \frac{T}{T^\circ} \right] \quad (11)$$

The dependence of equilibrium solubility on temperature is illustrated in Figure 1, which shows the natural logarithm of the equilibrium constant calculated using Eq. (11) plotted as a function of inverse temperature. The inclusion of heat capacity and its temperature dependence in the integral affects the predicted solubility constant curve by a small amount between 25° and 100°C as indicated by the minimal curvature.

It is evident from Figure 1 that the equilibrium solubility constant of schoepite increases with decreasing temperature from $10^{3.1}$ to $10^{4.8}$ between 100° and 25°C. This retrograde solubility is further illustrated by comparing the aqueous activity of UO_2^{2+} at different temperatures. At pH 8, $[\text{UO}_2^{2+}]$ at equilibrium with schoepite equals 6.48×10^{-12} at 25°C and 0.17×10^{-12} at 100°C. Total dissolved U concentrations would be much greater if U speciation is dominated by carbonate or other complexes as anticipated in the Yucca Mountain system. In a progressively cooling repository source term environment, the solubility of schoepite would progressively increase.

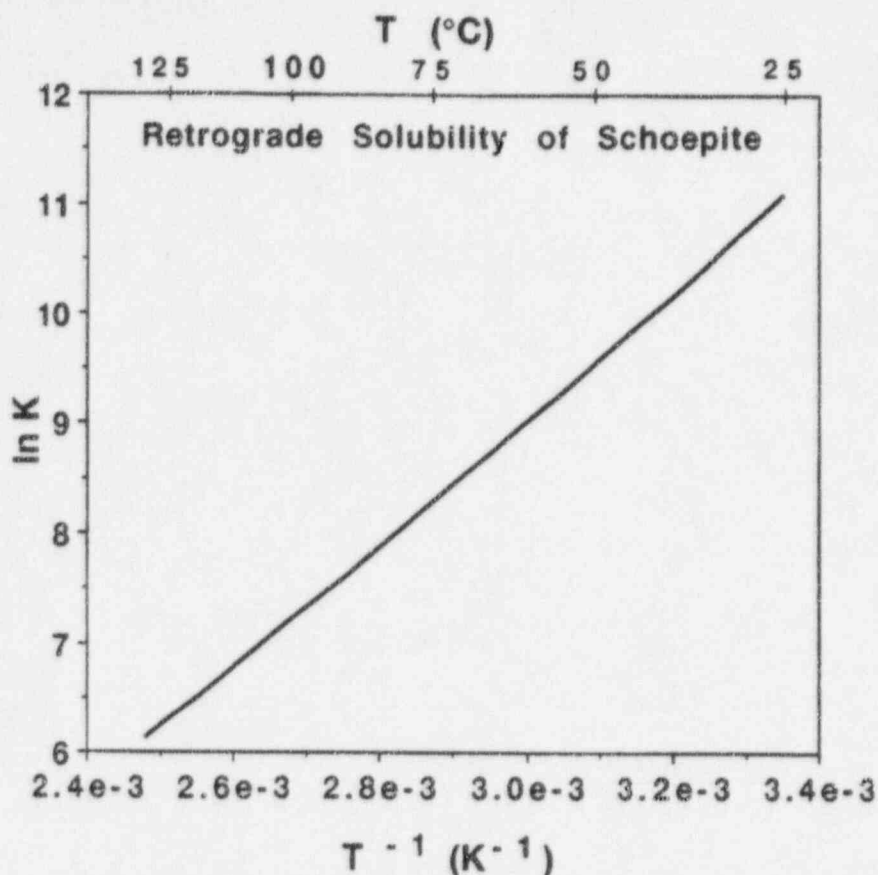
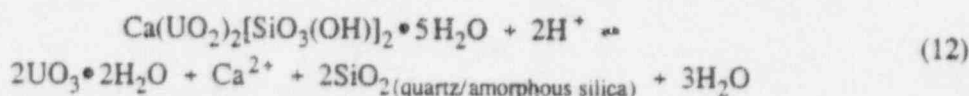


Figure 1. Natural logarithm of the equilibrium constant for the dissolution of schoepite (reaction 3) as a function of the inverse of the absolute temperature calculated using Eq. (11). Temperature in °C is given at the top of the figure.

Equilibrium between uranophane and schoepite can be expressed as



Reliable enthalpy and Gibbs free energy data are presently unavailable to perform a solubility analysis for uranophane. However, enthalpies for mineral transformation reactions that consume protons and release cations are typically negative. If the standard enthalpy of formation of uranophane is assumed to be close to that of schoepite plus quartz or amorphous silica and water, the enthalpy of reaction (12) would be dominated by the enthalpy of the Ca^{2+} ion, and its value would be negative. For these conditions, with decreasing temperature in the near field, schoepite plus a silica phase will be favored thermodynamically to form at the expense of uranophane despite the retrograde solubility of schoepite, which follows from the van't Hoff relation applied to reaction (12). These arguments suggest that the solubility of uranophane is also retrograde with temperature, even more strongly than schoepite solubility.

A mechanism that augments the retrograde solubility of uranyl minerals in general is the increasing stability of dominant aqueous uranyl carbonate complexes relative to uranyl plus bicarbonate with decreasing temperature between 200° and 25°C [11].

DISCUSSION

Interactions between water and uranyl minerals are likely to control the source term for U and other radioactive waste species at the proposed repository at Yucca Mountain. Solid solution has been observed in several natural uranyl silicates [6], Th has been noted as an impurity in uranophane [12], and Cs is largely included in secondary phases in experimental oxidative alteration of spent nuclear fuel [2]. The rate of release of U and other species will be controlled by a series of processes in which slow steps tend to control the overall rate. These processes include transport of oxidants and flux of water, oxidative dissolution of spent fuel, mineral precipitation (and coprecipitation), mineral dissolution or transformation, and radionuclide transport. If reaction and transport rates are sufficiently fast and solubilities are low, the system will approach equilibrium at the source; solubilities of secondary uranyl minerals limit concentrations of U and other waste species sequestered in these secondary phases; and the rate of dissolution will be controlled by the product of water flux and solubility. Such conditions would be favored by elevated temperatures relatively early in repository evolution. As solubilities increase with decreasing temperature, diffusion and reaction (e.g., oxidation and dissolution) rates decrease with decreasing temperature. For example oxidative dissolution of spent fuel in oxidizing Na carbonate/bicarbonate solutions follows Arrhenius behavior with an activation energy of 30 kJ/mole [13]. Increasing uranyl mineral solubilities and decreasing diffusion and reaction rates with decreasing temperature may lead to a change with time from solubility to transport, oxidation rate, or dissolution rate as the source term controlling mechanism in the cooling repository source area.

Preservation of large quantities of uranyl minerals formed by oxidation of uraninite and radiometric ages of secondary uranophane at the natural analog site at Peña Blanca [14] indicate that oxidative alteration was fast relative to transport of U away from the deposit [15]. Under oxidizing conditions in nature, uraninite alters to secondary uranyl minerals which tend to form in a sequence, such as uraninite \rightarrow schoepite \rightarrow soddyite \rightarrow uranophane, characterized by increasing incorporation of cations from the environment, e.g., [14]. However, the successive formation of schoepite, soddyite, and uranophane in natural settings may represent a paragenesis reflecting increasing temperature. In contrast, equilibrium solubility under conditions of decreasing temperature in a closed system, as described in relation to reaction (12), would lead to the reverse sequence. However, open system behavior is typical of alteration of rocks in the unsaturated zone at Yucca Mountain, where altered (zeolitized) rocks are commonly enriched in Ca and Mg relative to the primary bulk rock composition [16]. It is likely that environmental chemical conditions will also have a strong effect on formation of secondary uranyl minerals at Yucca Mountain.

Spent nuclear fuel oxidizes to U_4O_9 in moist air. At temperatures below 200°C this phase is apparently metastable, and complete oxidation in moist air to a U^{6+} phase does not occur over periods of time in excess of 4 yr under laboratory conditions [17]. However, in the presence of synthetic groundwater at 95°C, unirradiated UO_2 alters to secondary uranyl minerals including schoepite, soddyite, and uranophane [18]. Secondary products are also observed in long term spent fuel leaching tests designed to mimic conditions at a hypothetical Yucca Mountain repository [2]. In these tests it was concluded that a minimum of 70 to 90 percent of released gap and grain boundary ^{137}Cs was incorporated in these secondary phases. Secondary products have been observed in numerous other spent fuel and UO_2 alteration studies under oxidizing conditions (e.g., [19], [20], [21]). Experimental studies (as well as natural analog studies) indicate rapid formation of secondary phases relative to transport in systems relevant to Yucca Mountain. Liquid water is clearly necessary for formation of secondary phases that incorporate components such as Si or Ca from the geologic setting.

Liquid water is also required for transport of waste species out of the engineered barrier system (except for potential gas phase species such as ^{14}C). It is logical that spent nuclear fuel in the proposed repository at Yucca Mountain will react with liquid water to form secondary uranyl minerals prior to aqueous phase releases from the engineered barrier system by groundwater flow or aqueous diffusion. With a sufficient increase in the activity of aqueous Ca, uranophane may form rather than schoepite or soddyite despite diminishing temperature. Also, Fe derived from corrosion of waste container materials could affect the composition of secondary uranyl minerals in the repository near field. Uranyl is commonly found associated with ferric Fe in nature, e.g., at the Peña Blanca natural analog site [15].

CONCLUSIONS

The realistic evolution of the source area and near field environment at the proposed high-level nuclear waste repository at Yucca Mountain includes transformation of spent nuclear fuel to uranyl minerals, which would be the source term phases for uranium and much of the inventory of radioelements. Thermodynamic analysis indicates that uranyl minerals have retrograde aqueous solubilities. As the repository near field cools, solubilities of these source term phases will increase. This effect will be augmented by the increasing thermodynamic stability of dominant aqueous uranyl carbonate complexes with decreasing temperature. Retrograde solubility of source term phases, coupled with decreasing rates of transport and reaction with decreasing temperature, may lead to a change in the dominant source term mechanism from solubility to transport, oxidation, or dissolution rate in a cooling repository environment. Typical uranyl mineral paragenesis in natural analog systems indicate increasing incorporation of environmental components. However, this paragenesis is also consistent with prograde oxidation of primary uraninite. Open system interaction of the oxidation products of spent fuel with environmental components may stabilize more complex uranyl minerals despite stronger retrograde solubility characteristics.

ACKNOWLEDGMENTS

This article documents work performed by the Center for Nuclear Waste Regulatory Analyses (CNWRA) for the Nuclear Regulatory Commission (NRC) under Contract No. NRC-02-93-005. R.T. Pabalan, W.C. Patrick, C. Degueldre, B.W. Leslie, and two anonymous reviewers provided valuable suggestions on the text. The activities reported here were performed on behalf of the NRC Office of Nuclear Regulatory Research, Division of Regulatory Applications, and the NRC Office of Nuclear Material Safety and Safeguards, Division of Waste Management. The article is an independent product of the CNWRA and does not necessarily reflect the views or regulatory position of the NRC.

REFERENCES

1. W.M. Murphy, and E.C. Percy, in Scientific Basis for Nuclear Waste Management XV, edited by C.G. Sombret (Mater. Res. Soc. Proc. 257, Pittsburgh, PA, 1992) pp. 521-527.
2. P.A. Finn, J.C. Hoh, S.F. Wolf, S.A. Slater, and J.K. Bates, in Scientific Basis for Nuclear Waste Management XIX, edited by W.M. Murphy and D.A. Knecht (Mater. Res. Soc. Proc. 412, Pittsburgh, PA, 1996) pp. 75-81; *Radiochim. Acta* 74 pp. 65-71.

3. I. Grenthe, J. Fuger, R.J.M. Konings, R.J. Lemire, A.B. Muller, C. Nguyen-Trung, and H. Wanner, Chemical Thermodynamics of Uranium, edited by H. Wanner, and I. Forest (Elsevier Science Publishers B.V., Amsterdam, North-Holland, 1992).
4. I.R. Tasker, P.A.G. O'Hare, B.M. Johnson, G.K. Johnson, E.H.P. Cordfunke, *Can. J. Chem.* **66** (1988) pp. 620-625.
5. S.N. Nguyen, R.J. Silva, H.C. Weed, and J.E. Andrews, Jr., *J. Chem. Thermo.* **24** (1992) pp. 259-276.
6. I. Casas, J. Bruno, E. Cera, R.J. Finch, and R.C. Ewing, in Kinetic and Thermodynamic Studies of Uranium Minerals Assessment of the Long-Term Evolution of Spent Nuclear Fuel, (Swedish Nuclear Fuel and Waste Management Company, Technical Report 94-16, Stockholm, Sweden, 1994) p. 73.
7. H. Moll, G. Geipel, W. Matz, G. Bernhard, and H. Nitsche, *Radiochim. Acta* **74** pp. 3-7 (1996).
8. H.D. Holland and L.H. Brush, in Proceedings of the Conference on High-Level Radioactive Solid Waste Forms, edited by L.A. Casey, Nuclear Regulatory Commission, NUREG/CP-005, 1979, p. 597-615.
9. R.J. Finch, F.C. Hawthorne, and R.C. Ewing, in Scientific Basis for Nuclear Waste Management XIX, edited by W.M. Murphy and D.A. Knecht (Mater. Res. Soc. Proc. 412, Pittsburgh, PA, 1996) pp. 361-368.
10. R.C. Weast, CRC Handbook of Chemistry and Physics, edited by M.J. Astle, and W.H. Beyer, (CRC Press Inc., Boca Raton, Florida, 1988).
11. Based on the EQ3/6 data base data0.com.R2, Lawrence Livermore National Laboratory (1995).
12. C. Frondel, Systematic Mineralogy of Uranium and Thorium, (U.S. Geological Survey Bulletin 1064, Washington, DC: U.S. Government Printing Office, 1958).
13. W.J. Gray, H.R. Leider, and S.A. Steward, *J. Nuc. Mater.* **190** (1992) pp. 46-52.
14. E.C. Percy, J.D. Prikryl, W.M. Murphy, and B.W. Leslie, *App. Geochem.* **9** (1994) pp. 713-732.
15. D.A. Pickett, J.D. Prikryl, W.M. Murphy, and E.C. Percy, Submitted to *App. Geochem.* (1996).
16. D.E. Broxton, D.L. Bish, and R.G. Warren, *Clay Clay Min.* **35** (1987) pp. 89-110.
17. R.E. Einziger, L.E. Thomas, H.C. Buchanan, and R.B. Stout, *J. Nuc. Mater.* **190** (1992) pp. 53-60.
18. D.J. Wronkiewicz, J.K. Bates, T.J. Gerding, E. Veleckis, and B.S. Tani, *J. Nuc. Mater.* **190** (1992) pp. 107-127.
19. C.N. Wilson, in Scientific Basis for Nuclear Waste Management XIV, edited by T.A. Abrajano, Jr., (Mater. Res. Soc. Proc 212, Pittsburgh, PA, 1991) pp. 197-204.
20. Ch. Cachoir, M.J. Guittet, J.-P. Gallien, and P. Trocellier, *Radiochim. Acta* **74** (1996) pp. 59-63.
21. R. Taylor, R.J. Lemire, and D.D. Wood, in High Level Radioactive Waste Management, (Amer. Nuc. Soc., La Grange Park, IL, 1992) pp. 1,442-1,448.